Twentieth Symposium (International) on Combustion/The Combustion Institute, 1984/pp. 2073–2082

A MODEL OF COMBUSTION MONOPROPELLANTS (AP) WITH COMPLEX GAS PHASE KINETICS

H. K. NARAHARI, H. S. MUKUNDA, AND V. K. JAIN
Department of Aerospace Engineering
Indian Institute of Science
Bangalore-560 012, India

The results of a model of the combustion of monopropellants, using ammonium perchlorate as the specific example and treating the complex gas phase kinetics and diffusion by the trace diffusion approximation, are presented in this paper. The species considered are $HClO_4$, NH_3, ClO_3, NH_2, ClOH, HNO, Cl, O, NO, N_2O, N_2, Cl_2, ClO, HCl, O_2 and H_2O, and are expected to participate in 14 reversible reactions. Kinetic data for the reactions are based on the works of Ermolin,[5] Guirao, and Williams[1] and Jacobs and Pearson.[18] The time-dependent governing equations are solved by the method of lines, and the results for mass burn rate, pressure index and temperature sensitivity are compared with those of experiments. Some perturbational calculations show that inclusion of NO_2 and ClO_2, in palce of atomic oxygen, leads to more realistic predictions for mass fractions and burning rate.

Introduction

Combustion of solid monopropellant like, ammonium perchlorate [AP] has been modelled by several researchers.[1–4] Most of these studies have assumed single-step kinetics for the gas-phase reaction. Guirao and Williams[1] have also treated the problem by using single-step gas phase kinetics but deduced the kinetic parameters by analysing an assumed chain mechanism under isothermal and isobaric conditions. The assumption of a rate controlling overall reaction leads implicitly to a pressure index for the reaction rate of second order, resulting in a larger burn rate pressure index than that observed experimentally (~0.77). In fact, the analysis of Beckstead[2] et al has established a rather simple formalism which is essentially equivalent to that of Guirao and William,[1] and leads to the correct pressure index only when the reaction rate is of order 1.8. The only way in which the pressure index of the burn rate can be predicted is to treat the gas phase kinetics in detail. Ermolin et al[5] have computed the flame structure of AP with complex kinetics. Their theory ignores both thermal conduction and diffusion. While the basic elements of their theory do not preclude calculation of the mass flux ($\dot{m}''$), they have not made any such calculation and seem to indicate that the mass flux is the same for a range of pressures. The present authors are aware of no study which solves the conservation equations with complex kinetics and realistic diffusion and obtains combustion characteristics, including mass burn rate. The present paper therefore addresses itself to the solution of the problem of linear regression of a monopropellant with complex gas phase kinetics and trace diffusion. While the basic framework is applicable to any monopropellant, the treatment presented here takes account of some of the freatures of combustion specific to AP, HMX, RDX. The reason for going into these complexities is to set up a model by which one can examine the importance of gas phase kinetics. The effect of catalysts (burning rate modifiers) can also be studied by considering their effect on various reaction steps in so far as the effect on gas phase kinetics is considered. Experimentally it has been observed[6–8] that the surface of the combusting solid in the above cases has a liquid layer. In the specific case of AP it has been deduced[2] that reactions take place in the liquid layer effectively neutralising the endothermicity of decomposition of AP and even making the situation at the surface exothermic. The present theory as distinct from all the earlier theories takes explicit account of the liquid layer and allows the interface regions to be endothermic/exothermic as dictated by specific situations. If one considers the class of monopropellants which do not show a surface melt layer, it is simple matter to incorporate the necessary changes. They are included in the text at the appropriate places. In the following sections the formulation of the problem, method of solution and the results of the computation are described. Comparison of results for AP with those of experiments are also presented.

Formulation

The formulation of the problem calls for the enunciation of the governing equations for the gas phase and the condensed phase along with the interface conditions. The governing equations for the gas phase for the case of (N − 1) chemical species reacting in R steps for the plane one dimensional case are:

$$\rho_t + (\rho u)_x = 0 \tag{1}$$

$$\rho(Y_n)_t = (D_n \rho (Y_n)_x)_x - \rho u (Y_n)_x + \dot{\omega}_n''', \quad n = 1, N-1 \tag{2}$$

$$\rho \bar{c}_p T_t = ((T)_x)_x - \rho \bar{c}_p u (T)_x - \sum_{n=2}^{N} h_n \dot{\omega}_n''' + \sum_{n=1}^{N} D_n (Y_n)_x (T)_x c_{p_n} \tag{3}$$

$$Y_N = 1 - \sum_{n=1}^{N-1} Y_n \tag{4}$$

$$P = \rho RT/\bar{M}, \quad \bar{M} = \left(\sum_{n=1}^{N} Y_n / M_n \right)^{-1} \tag{5}$$

$$h_n = h_n^0 + \int_{T_{ref}}^{T} c_{p_n} dT; \quad \bar{c}_p = \sum_{n=1}^{N} c_{p_n} Y_n \tag{6}$$

here $(T)_x = \partial T/\partial x$ and $(Y_n)_x = \partial Y_n/\partial x$ etc.

The unsteady state formulation, given here has been chosen instead of the steady state formulation because of the inherrent computational advantages in treating unsteady conservation equations. Also physically realistic oscillatory solutions if present are extracted from the solution of the above equations. Use of the transformation $\psi_x(x, t) = \rho(x, t)$ automatically satisfies the continuity equation. The species conservation and energy equations can now be written as

$$(Y_n)_t = (D_n \rho^2 (Y_n)_\psi)_\psi - \dot{m}_o''(Y_n)_\psi + \dot{\omega}_n'''/\rho \tag{7}$$

$$(T)_t = (k\rho(T)_\psi)_\psi/\bar{c}_p - \dot{m}_o''(T)_\psi - \sum_{n=1}^{N} h_n \mathring{\omega}_n'''/\rho \bar{c}_p + \rho^2/\bar{c}_p \sum_{n=1}^{N} D_n c_{p_n} (T)_\psi (Y_n)_\psi \tag{8}$$

where $\dot{m}_o'' = \rho_p r$ refers to the mass flux from the surface ($x = 0$). The reaction rates $\dot{\omega}_n'''$ are given by the classical law of mass action as

$$\mathring{\omega}_n''' = M_n \sum_{r=1}^{R} (\nu_{nr}'' - \nu_{nr}') \left[R_{k_f} \prod_{n=1}^{N} \left(\frac{Y_n}{M_n \rho} \right)^{\nu_{nr}'} - R_{k_b} \prod_{n=1}^{N} \left(\frac{Y_n}{M_n \rho} \right)^{\nu_{nr}''} \right] \tag{9}$$

where R_{k_f} and R_{k_b} refer to forward and backward specific reaction rates, M_n is the molecular weight of nth species and ν_{nr}' and ν_{nr}'' are stoichiometric coefficients. The reaction rates refer to the reaction equation

$$\sum_{r=1}^{R} \sum_{n=1}^{N} \nu_{nr}' A_n \rightleftarrows \sum_{r=1}^{R} \sum_{n=1}^{N} \nu_{nr}'' A_n \tag{10}$$

The diffusion coefficients are evaluated using the trace diffusion approximation. This was first proposed by Hirschfelder[14] and has been extensively used for flame propogation calculations subsequently. This model is exact for binary mixtures and for trace species and is a good approximation for the general case. The only possible objection against this is that it violates the species conservation law in a mixture (because the mass fractions of all species do not add up to unity, errors are introduced in the 5th or 6th decimal place).

Other studies by Spalding[15] and Stephenson[16] have shown it to be a reasonable approximation for flame speed calculations and hence the same approximation is taken to be valid in the present calculations.

The diffusion coefficient is obtained from the equation

$$D_j = \frac{(1 - Y_j)}{\sum_{k \neq j} \frac{X_j}{D_{jk}}} \tag{11}$$

where D_{jk} is the binary diffusion coefficient.

The governing equations of the condensed phase are now discussed. Figure 1 shows schematically the features of the condensed phase schematically. The solid phase occupies the region $-\infty \leq x \leq -\delta_1$, where δ_1 is the thickness of the liquid layer. The region $-\delta_1 \leq x \leq 0$ is occupied by the liquid layer. The region above $x = 0$ is the gas phase. All changes of heat are expected to take place at interfaces only. No bulk reactions in the solid or liquid layer are permitted in the present analysis. Treating the condensed phase processes as quasi-steady, the equations are

$$(k_i(T_i)_x)_x - \dot{m}_o'' c_{p_i}(T_i)_x = 0 \quad i = S, L \tag{12}$$

If there is no liquid layer, the equation corresponding to $i = L$ is to be omitted.

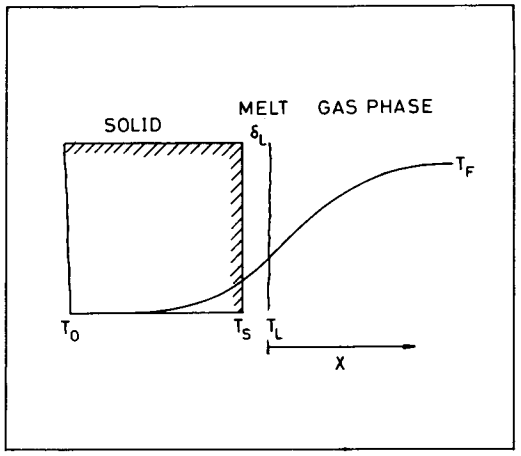

FIG. 1. Schematic of the model.

The Boundary, Interface and Initial Conditions

$$T(-\infty, t) = T_o;\ T(-\delta_1, t) = T_s \text{ (fusion temperature)} \quad (13,14)$$

$$k(T)_x]_{x=-\delta_l^+}^{x=-\delta_l^-} = \dot{m}_o'' Q_S;\ k(T)_x]_{x=0^-}^{x=0^+} = \dot{m}_o'' Q_L \quad (15,16)$$

$$D_n \rho (Y_n)_x]_{x=0^+} = \dot{m}_o''(Y_n - Y_n^-) \quad (17)$$

$$x \to \infty \Rightarrow (Y_n)_x,\ (T)_x \to 0 \quad (18)$$

In the above equations Q_S and Q_L refer to heats of phase change (Solid to liquid) and exothermic/endothermic liquid to gas phase change. Y_n^- refers to mass fractions of species on the liquid side of the interface. They are given by

$$Y_{HClO_4}^- = M_{HClO_4}/M_{AP},\ Y_{NH_3}^- = M_{NH_3}/M_{AP} \quad (19)$$

and zero for the rest of the Y_n^- s.

Transformations

For the sake of computational ease the governing equations are transformed to

$$\tau = (T - T_o)/(T_f - T_o); \quad (20)$$

$$z = (\psi - \psi_o)/(\psi_f - \psi_o), \quad (21)$$

$$t^* = t/\bar{t} \quad (22)$$

so that the zone of integration for t and z are between 0 and 1, where ψ_f and ψ_o are constants. The equations are

$$(Y_n)_{t^*} = \bar{t}(D_n \rho^2 (Y_n)_z)_z/(\psi_f - \psi_o)^2 - (Y_n)_z \dot{m}_o'' \bar{t}/(\psi_f - \psi_o) + \bar{t}\dot{\omega}_n'''/\rho,\ n = N - 1 \quad (23)$$

$$(\tau)_{t^*} = \bar{t}/(\bar{c}_p(\psi_f - \psi_o)^2)\ (k\rho(\tau)_z)_z - \dot{m}_o''\bar{t}/(\psi_f - \psi_o)(\tau)_z - \bar{t}/(\bar{c}_p(T_f - T_o)) \cdot \left[\sum_{n=1}^{N} h_n \dot{\omega}_n'''/P\right] + \rho^2 \bar{t}/(\bar{c}_p(\psi_f - \psi_o)^2) \cdot (\tau)_z \sum_{n=1}^{N} D_n c_{p_n} (Y_n)_z \quad (24)$$

In the above equations $(\psi_f - \psi_o)$ is chosen from the relation $\psi_f - \psi_o = \int_o^{x^*} \rho(x)dx$ where x^* is the thickness of the flame zone. Estimates from experimental measurements (~100 μm) are used as a rough guide to set a value for $(\psi_f - \psi_o)$.

The initial conditions in the gas phase need to be specified for the mass fractions of various species and temperature at $z = 1$ ($x \to \infty$), these are given by equilibrium considerations. For the given monopropellant, the adiabatic flame temperature (T_f) and equilibrium composition are calculated at each of the pressures and these values are set at $z = 1$ (large x). The variation of the mass fractions are treated as linear functions of τ for major species and quadratic functions for minor species and τ vs z is given by

$$\tau = \left[\frac{\tau_L \exp\left(\dfrac{\dot{m}_o'' \bar{c}_p(\psi_f - \psi_o)}{k} \cdot z\right)}{1. - \tau_L \exp\left(\dfrac{\dot{m}_o'' c_p(\psi_f - \psi_o)}{k} \cdot z\right)}\right] \quad (25)$$

where τ_L corresponds to liquid surface temperature. This is essentially an exact solution for a simple reaction rate function.[12,13] Since the integration involves excessive computer time, what is actually done is to first obtain converged results for a control set of parameters (P = 45 atm, T_o = 300 K) and then use these as input profiles for futher work.

$$\dot{m}_o'' = A_L \exp(-E_L/RT_L) \quad (26)$$

Here the value of the activation energy E_L chosen is the now generally accepted value[10] of 125.52 kJ/mole. The choice of frequency factor A_L however merits discussion. The presence of a melt layer on the deflagrating strands of AP has been established. The interface temperature between solid and liquid has been shown to be invariant with respect to pressure and has been estimated to be 865 ± 20 K.[8,9] Low pressure extinction studies have shown

that the burning rate at extinction does not change (~5.85 kg/m^{2}s) with initial temperature although the low pressure deflagration limit (LPDL) itself is dependent on the initial temperature. Consistent with the presently accepted hypothesis that extinction occurs when the liquid layer vanishes (or $T_s \leq$ 865 K), the value of A_L is chosen so as to yield the observed mass burning rate (at extinction) when the liquid surface temperature is equal to 865 K.

The Method of Solution

The governing equations can essentially be written in the form

$$(\phi_i)_t = a_i(A_i(\phi_i)_z)_z - b_i(\phi_i)_z + RR_i, \quad i = 1, N \quad (27)$$

where $i = 1$ refers to temperature and others to species as already noted. The term RR_i includes all the source terms.

In order to solve the above equations the method of lines[17] is adopted. The spatial coordinate spanning from 0 to 1 is split into a number of segments ($j = 1$, NSEG). The right side of Eq. (27) is differenced by using a second order central difference scheme. The difference equation thus obtained is

$$(\phi_i)_t = \frac{a_i}{\Delta z^2}\left[A_{i,j+1/2}(\phi_{i,j+1} - \phi_{i,j}) - A_{i,j-1/2}(\phi_{i,j} - \phi_{i,j-1})\right] - \frac{b_i}{2\Delta z}[\phi_{i,j+1} - \phi_{i,j-1}] + RR_{i,j} \quad (28)$$

where $A_{i,j+1/2}$ refers to the mean of $A_{i,j}$ and $A_{i,j+1}$. This difference equation when written for the sur-

TABLE I
Input data for reaction mechanism

Sl. No.	REACTION STEP	Log_{10} A	α	E(kJ/mole)	SOURCE Ref.
1.	$HClO_4 \rightarrow OH + ClO_3$	11.0	0.00	163.4	5
2.	$ClO_3 + M \rightarrow ClO + O_2 + M$	12.23	0.50	0.0	5
3.	$NH_3 + OH \rightarrow NH_2 + H_2O$	12.52	0.00	9.2	19
4.	$NH_3 + ClO \rightarrow NH_2 + ClOH$	11.62	0.50	26.8	5
5.	$NH_3 + Cl \rightarrow NH_2 + HCl$	11.65	0.50	0.4184	5
6.	$NH_2 + O_2 \rightarrow HNO + OH$	13.71	0.00	126.4	19
7.	$NH_2 + NO \rightarrow N_2 + H_2O$	19.95	−2.46	7.53	19
8.	$HClO_4 + HNO \rightarrow ClO_3 + NO + H_2O$	13.48	0.00	25.1	5
9.	$ClOH + OH \rightarrow ClO + H_2O$	13.26	0.00	0.0	5
10.	$2NO \rightarrow N_2O + O$	12.11	0.00	134.3	5
11.	$ClO + O \rightarrow Cl + O_2$	13.82	0.00	1.84	5
12.	$2ClO \rightarrow Cl_2 + O_2$	11.30	0.00	0.0	5
13.	$HClO_4 + Cl \rightarrow ClOH + ClO_3$	12.08	0.00	34.5	5
14.	$2Cl + M \rightarrow Cl_2 + M$	14.86	0.00	−7.5	5

Specific reaction rate is given by the expression $R_k = AT^{\alpha} \text{ Exp } (-E/RT)$.

TABLE II
Input parameters for different species

Sl. No.	Species	Mol. Wt.	Heat of Formation (kJ/mole)	σ (Anstroms)	ϵ/k (k)	Reference
1.	$HClO_4$	100.50	−10.46	1.800	452.0	*a*
2.	NH_3	17.00	−46.0	2.900	558.3	16
3.	ClO_3	83.45	154.8	3.842	184.0	*b*
4.	ClO	51.45	101.2	3.842	184.0	16
5.	NH_2	16.00	167.8	2.900	558.3	16
6.	ClOH	52.45	−92.0	3.842	184.0	*b*
7.	HNO	31.00	99.6	3.470	119.0	16
8.	OH	17.00	39.3	3.147	79.0	16
9.	Cl	35.45	121.0	3.613	130.8	16
10.	0	16.00	249.4	3.065	106.7	16
11.	NO	30.00	90.4	3.492	116.7	16
12.	N_2O	44.00	82.0	3.816	237.0	15
13.	N_2	28.00	0.0	3.681	91.5	15
14.	Cl_2	70.90	0.0	4.217	316.0	15
15.	HCl	36.45	−92.0	3.305	360.0	15
16.	O_2	32.00	0.0	3.499	100.0	15
17.	H_2O	18.00	−242.0	2.641	809.1	15

a. σ and ϵ/k estimated from melting and boiling temperatures (Eqn. 2–3, Ref 22).
b. σ and ϵ/k values taken same as for ClO for which it is available.

face node ($j = 1$) contains a false point $\phi_{i,-1}$. This is treated by using a central difference operator at the boundary interface conditions and eliminating the false point. For example

$$(\tau)_z|_{j=1} = (\tau_2 - \tau_{-1})/2\Delta z \Rightarrow \tau_{-1} = 2(\tau)_z|_{j=1}\,\Delta z$$

here $(\tau)_z|_{j=1}$ is obtained from Eq. (15).

The above set of ordinary differential equations can be handled by ODE solvers like Runge-Kutta-Gill Package or Hindmarch-Gear.[20] In the present work, the Hindmarch-Gear code (Gear B) was used with stiff option.

The Chain Mechanism

The detailed kinetics chosen are presented in Table I. The kinetic parameters used in the present work are taken from sources identified in Table I. While the number of species (N), as well as the number of chemical steps, can be increased, the results presented here refer to (N = 17) and (R = 14) reversible steps.

The overall mechanism that has been chosen is similar to the one proposed by Jacobs and Pearson.[18] Some of the reactions have been replaced by others cited by Ermolin et al[5] based on plausibility

arguments. While it would have been possible to take into account more reactions, in view of the computational limitations, as well as the need to obtain experience in handling combusting solids, the limited set was chosen. The forward rate constants are the same as cited in references[5,19] and the backward rate constants were obtained by dividing the forward rate constant by the equilibrium constant which itself is obtained from thermodynamic data of the various species, available in the JANAF[23] tables. The seventeen species considered, along with the basic parameters needed for obtaining diffusion coefficients, are listed in Table II. Some properties like c_p, σ_a, ϵ/k for the species $HCLO_4$, CLO_3 and CLOH are not available and they are tentatively assumed to be the same properties as for CLO. Thermal conductivity, viscosity and diffusion coefficients are calculated using the formulae given in Brokaw's[21] report. The data of condensed phase is shown in Table III.

TABLE III
Input parameters for condensed phase

Sl. No.	Name	Value used
1.	Density (kg/m^3)	1950.0
2.	C_s (kJ/kg mole °K)	1.51
3.	Thermal conductivities (W/m °K)	0.42
4.	Adiabatic Flame Temperature (°K)	1400.0
5.	Heat of phase Q_s change (kJ/kg)	356.0
6.	Solid-Liquid (melt) interface temperture (°K)	865.0
7.	Heat of phase change at liquid gas interface Q_L (kJ/kg)	502.0
8.	Activation energy of Pyrolysis E_L (kJ/mole)	125.52
9.	Frequency factor of Pyrolysis law A_L (See text)	2.23×10^7

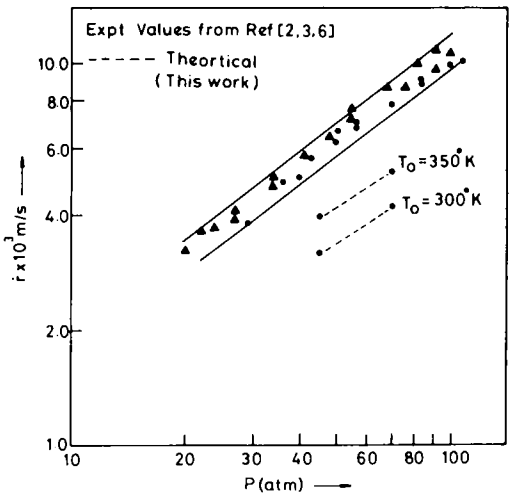

FIG. 2. Burning rate of AP at different pressures.

Results and Discussion

The calculation procedure programmed on the DEC-1090 computer took about 45 minutes of CPU for the first convergence. Convergence is assumed

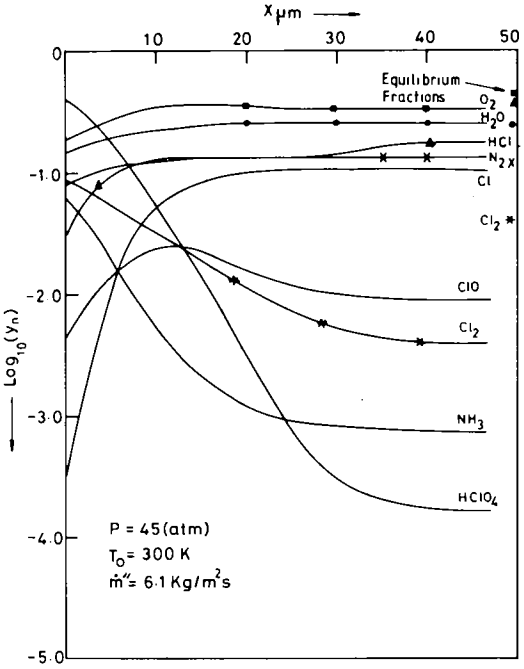

FIG. 3. Variation of mass fractions with distance.

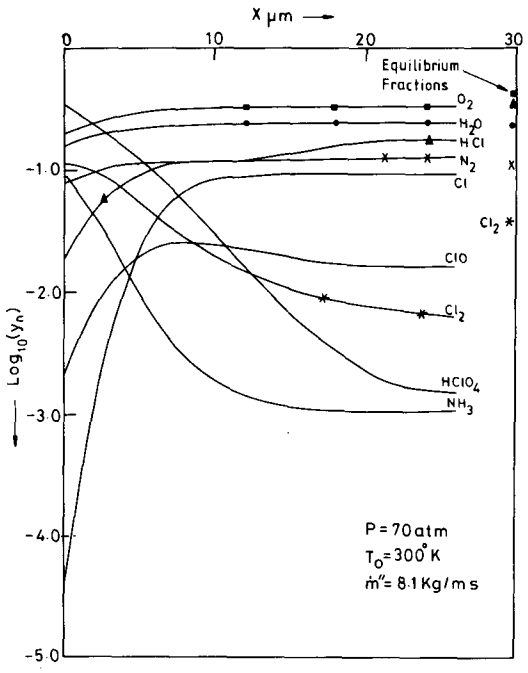

FIG. 4. Variation of mass fractions with distance.

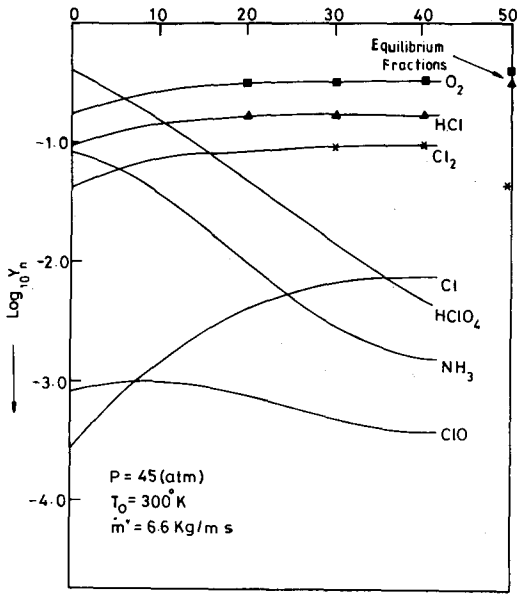

FIG. 5. Variation of mass fractions with distance for modified reaction mechanism.

to have taken place when the maximum time gradients are at least one order lower than the minimum of the others, and concentrations, temperature and mass burn rate do not change by more than 1%. The latter criterion was not as hard to satisfy as the former, although they are essentially equivalent. The calculations could be completed for two pressures and initial temperatures; perturbational calculations have been completed for several cases.

The results of the calculations are shown in Figs. 2–5 and Table IV. The linear burn rate vs pressure shown in Fig. 2 indicates that the burn rates obtained from the present calculations are substantially lower than the experimental results. The burn rate index is 0.67 and σ_p, the temperature sensi-

TABLE IV

Sl. No.		P = 45 atm.		P = 70 atm.		Pres Index γ	Temp sensitivity %/°C
		T_0 = 300° K	T_0 = 350° K	T_0 = 300° K	T_0 = 350° K		
1.	Experimental Mass Burn Rates kg/m^{2}s	11	12	15.2	16.8	0.77	0.2
2.	Computed Mass Burn Rates kg/m^2 s	6.1	7.5	8.2	10.2	0.67	0.4
3.	Mass burn Rates for Modified Reaction Scheme kg/m^2 s	6.6					

tivity is 0.4%. The experimental values are 0.77 and 0.2%. The results of the present computation, particularly with respect to the pressure index, indicate that the decomposition of $HClO_4$, i.e. the only first order reaction, must be rate controlling. The temperature sensitivity (σ_p) which can be roughly taken as proportional to $E_g/2RT_f^2$ where E_g is the gas phase activation energy, indicates again that the first reaction has a significant influence on the value of σ_p ($45000/2 \times 1.98 \times 1400^2 \sim 0.58\%$).

These differences also seem to exhibit themselves in the results of mass fraction profiles shown in Fig. 3 and 4 for pressures of 45 atm and 70 atm. These figures, which show the variations of mass fractions of most species with distance, indicate that the thickness over which these variations take place is about 50 μm for 45 atm and 26 μm for 70 atm. The mass fractions reach the equilibrium mass fractions in the case of H_2O, O_2 and N_2. The mass fractions of HCl, Cl_2 and Cl are significantly different. In particular, Cl_2 is lower than the equilibrium fraction and Cl is significantly larger.

The fact that exponent 0.67 is smaller than the observed value was to the dominance of the first order decomposition kinetics of $HClO_4$. For the exponent to be larger, the importance of the reactions with second or third order kinetics must be increased. An examination of the kinetic data of Ermolin[5] shows that the rate constants of $HClO_4 + Cl \rightarrow ClOH + ClO_3$ (reaction 13 in Table I) cannot be traced to any experimental source. Suspecting that the kinetic data provided may not be appropriate, the result with frequency factor multiplied by 10 was used. However, this did not show any significant difference in the burn rate. Calculations at pressures of 40 atm showed that the liquid surface temperature dropped below the minimum temperature of 865° K (the low pressure deflagration limit, LPDL). This implies that for the present kinetic data, LPDL is about 40 atm instead of 20 atm.

Thus the present model seems to offer features which are all consistent among themselves, but the final results obtained are at variance with experimental values.

Modelling studies[2,3,13] seem to indicate that the activation energy of the pyrolysis has only a marginal effect on the pressure index, as well as on the temperature sensitivity which is controlled to a large extent by the gas phase kinetics. In fact, as long as the gas phase parameters are unchanged, results based on either Pyrolysis or the Equilibrium condition at the surface seem to be the same. Hence the only set of data which has a significant impact are the gas phase kinetic data. Since this is the first set of calculations with the available published kinetic data, it appears that there is a need to re-examine the data more carefully.

TABLE V

Reactions dropped	10	$2NO \rightarrow N_2O + O$
	11	$ClO + O \rightarrow Cl + O_2$
New reactions included are		$NO + CLO \rightarrow Cl + NO_2$
		$2HNO \rightarrow H_2O + N_2O$
		$HNO + O_2 \rightarrow NO_2 + OH$
		$Cl + O_2 + M \rightarrow CLO_2 + M$
		$ClO_2 + Cl \rightarrow 2CLO$
		$2NO_2 \rightarrow O_2 + 2NO$

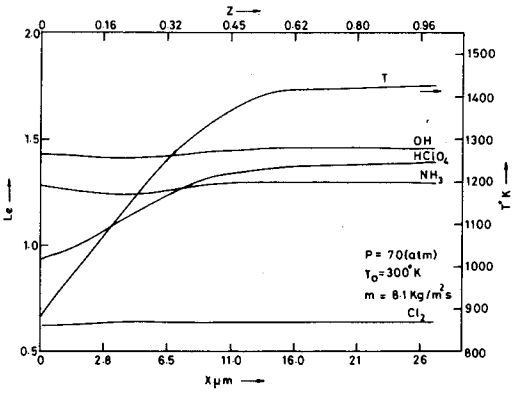

FIG. 6. Variation of Lewis number and temperature with distance.

One cause may be the limited set of species and reactions chosen from a vast number of possibilities (e.g. 85 reactions steps are proposed by Ermolin). Both NO_2 and ClO_2 were included in place of atomic oxygen which was found to be present in a very small quantity. The reaction mechanism was also modified keeping in mind the above changes. Table V gives the new reactions together with the old reactions which were dropped.

Figure 5 is a plot of the mass fractions with distance for the modified scheme. The improvement over the results of the previous scheme shown in Fig. 3 is quite obvious. The mass fractions of radicals Cl and ClO which were unacceptably high are now more realistic. The mass fraction of Cl_2 is also nearer to the final equilibrium value. The improvement over the earlier mass burning rate ($\dot{m}''_{new}$ = 6.6 kg/m^{2}s) is however not as satisfactory even though the direction of change is correct. In essence, work still needs to be done before one can obtain a good comparison between the experimental and theoretical results.

Figure 6 is a plot of the variation of the Lewis number with distance. As can be seen, the deviations of the Lewis number from unity is not large, although not insignificant. This figure is included to emphasize this point, since supposed deviations of the Lewis number from unity are presented as the

reason for some observed features of AP combustion.[20]

Conclusion

The problem of combustion of Solid Monopropellants has been tackled numerically using detailed gas phase kinetics, realistic diffusion and a melt layer on the deflagrating surface. Calculations with AP as a specific case are presented. Kinetic data from available sources have been used throughout. The predictions from the calculations show (a) lower burning rate, (b) higher temperature sensitivity, and (c) higher LPDL. The causes for these have been hypothesized, but detailed calculations to assess their relative importance are underway. However, preliminary calculations indicate the correctness of the hypothesis. An interesting feature observed during the calculations was that the Lewis numbers for different species were not very different from unity. This is in contrast to an earlier suggestion[20] that the large difference in diffusivities between NH_3 and $HClO_4$ could lead to the formation of cellular flames.

Nomenclature

A Frequency factor.
$\bar{C}_p$ Mixture specific heat (kJ/kg °C).
C_{p_n} Specific heat of n^{th} species (kJ/kg °C).
D_n Diffusion coefficient using trace approximation (m^2/s).
E Activation energy (kJ/kg mole °K).
h Enthalpy of mixture (kJ/kg).
h_n Enthalpy of n^{th} species (kJ/kg).
J Grid index in the spatial direction.
k Thermal conductivity (W/m °K).
L_{en} Lewis number of n^{th} species ($D_n\rho\bar{c}_p/k$).
M Molecular weight.
$\dot{m}''$ Mass burning rate (kg/m^2s).
N Total number of partial differential equations.
n Index used for species.
P Pressure (atm).
Q_s Heat absorbed at solid-liquid interface (kJ/kg).
Q_l Heat released at liquid-gas interface (kJ/kg).
R_k Specific reaction rate.
R Universal gas constant.
RR Source term in Eq. 25.
r Linear burning rate (m/s).
T Temperature (°K).
t Time (s).
$\bar{t}$ Time scaling factor (1×10^{-8} s).
$\dot{\omega}'''$ Reaction rate.
x Distance (μm).
Y Species.
z Transformed nondimentional variable.
α Temperature power index.
γ Burning rate power index.
δ_1 Melt layer thickness (μm).
ψ Transformation variable ($= \int \rho\, dx$).
τ Non-dimentional temperature.
ρ Mixture density (kg/m^3).
ρ_p AP crystal density (kg/m^3).
ν Stoichiometric coefficient.

Subscripts

o Initial condition.
S Solid phase.
F Flame.
L,l Liquid Layer.

Acknowledgment

One of the authors, H. K. Narahari, would like to thank the authorities of the Aeronautical Research and Development Board (ARDB) for financial support during the period of this work.

REFERENCES

1. Guirao, C. and Williams, F. A.: AIAAJ, 9, p 1345 (1971).
2. Beckstead, B. W., Derr, R. L.: and Price, C. F.: Thirteenth Symposium (International) on Combustion, p 1047, Combustion Institute, Pittsburgh, PA (1970).
3. Price, C., Boggs, T., and Derr, R. L.: AIAA 16th Aerospace Sciences Meeting, 78-219, Alabama (1978).
4. Miller, M. S.: Combustion and Flame, 46, p 51 (1982).
5. Ermolin, N. E., Korobeinichev, O. P., Tereshcenko, A. G., and Fomin, V. M.: Combustion, Explosion and Shock Waves, 18, p 61 (1982).
6. Taylor, J. W.: Combustion and Flame, 6, p 15 (1962).
7. Hightower, J. D., and Price, E. W.: Eleventh Symposium (International) on Combustion, p 463, Combustion Institute, Pittsburgh, PA (1967).
8. Cords, H. F.: AIAAJ, 7, p 1193 (1965).
9. Beckstead, M. W., and Hightower, J. D.: AIAAJ, 5, p 1985 (1967).
10. Jacobs, P. W. M., and Whitehead, H. M.: Chemical Reviews, p 551 (1969).
11. Benreuven, M., Caveny, L. H., Vichnevetsky, R. J., and Summerfield, M.: Sixteenth Symposium (International) on Combustion, p 1223, Pittsburgh, PA (1976).
12. Spalding, D. B.: Combustion and Flame, 1, p 296 (1957).
13. Narahari, H. K., Mukunda, H. S., and Jain, V. K.: communicated to Combustion and Flame Journal.

14. HIRSCHFELDER, J. O. AND CURTIS, C. F.: third Symposium (International) on Combustion, p 121 (1949).
15. SPALDING, D. B., STEPHENSON, P. L., AND TAYLOR, R. G.: Combustion and Flame, 17, p 55 (1971).
16. STEPHENSON, P. L., AND TAYLOR, R. G.: Combustion and Flame, 20, p 231 (1973).
17. BLEDJIAN, L.: Combustion and Flame, 20, p 5 (1973).
18. JACOBS P. W. M., AND PEARSON, G. S.: Combustion and Flame, 13, p 419 (1969).
19. DEAN, A. M., HARDY, J. E., LYON, R. K.: Nineteenth Symposium (International) on Combustion, p 97, Pittsburgh, PA (1982).
20. EDWARD MCHALE, T., AND VON ELBE, GUENTHER: Combust Science and Tech. 2, p 227 (1970).
21. HINDMARSH, A. C.: GEARB-Solution of ordinary Infferential Equations having Banded Jacobian, Lawrence Livermare Laboratory Report UCID-30059 Rev. 2 (1977).
22. BROKAW, R. C.: Alignment charts for Transport Properties, Viscosity, Thermal Conductivity and Diffusion Coefficient for Non-Polar Gas Mixtures at low density, NASA TR-R81 (1961).
23. SVEHLA, R. A.: Estimated Viscosities and Thermal Conductivities of Gases at high temperatures, NASA TRR 132 (1962).
24. JANAF, Thermochemical Tables, Nat. Bua. Stand. (1965).